

# Impact of Molarity on the Structural, Morphological and Optical Properties of CeO<sub>2</sub> Thin Films Prepared by Spray Pyrolysis Technique

Hamed A. Gatea<sup>1,2</sup> and F. K. Hachim<sup>3,\*</sup>

<sup>1</sup>Department of Medical Physics, Al-Mustaqbal University College 51001, Hillah, Babylon, Iraq

<sup>2</sup>Directorate Education of Thi Qar, Thi Qar, Iraq

<sup>3</sup>Physics Department, College of Science, Thi-Qar University, Thi-Qar, Iraq

Received: 21 Sep. 2022, Revised: 22 Oct. 2022, Accepted: 20 Nov. 2022.

Published online: 1 Jan. 2023

**Abstract:** CeO<sub>2</sub> thin films are deposited on glass substrate by spray pyrolysis technique (SPT) at 623 K using different molar concentration of cerium chloride precursor solution. The structural, morphological and optical properties of films were investigated by a set of characterization techniques such as X-ray diffraction (XRD), scanning electron microscopy (SEM), UV-VIS-IR. The estimation of crystallite size is 80-120 nm, which is confirmed by Scherer formulae from XRD pattern. XRD analysis shows that the film has cubic fluorite phase with orientation along (111) for all molarity. The optical energy gap decreased with the increase of crystallite size (98-120 nm) due to the size effect.

**Keywords:** Molar concentration, CeO<sub>2</sub> films, morphology, structure, Optical properties, crystal size.

## 1 Introduction

Thin-film deposition using metals materials have received more attention by researchers owing their enhanced electrical, magnetic and optical properties, for desirable applications [1-3]. Among the materials, Ceria (CeO<sub>2</sub>) is a well-known material and CeO<sub>2</sub> film has unique properties which is well suitable for various biological and engineering applications. It exhibits good transmission in the infrared and visible region with high refractive index and wide optical energy gap of 3.4-3.6 eV [4-6].

Due to strong adhesion to surface between CeO<sub>2</sub> film and substrate, spray pyrolysis (SP) technique is used to deposit CeO<sub>2</sub> films on glass substrate [5]. These thin film of CeO<sub>2</sub> deposited on glass substrate exhibits high stability against chemical erosion and mechanical abrasion [6,7]. The structure of CeO<sub>2</sub> film showed face centered cubic structure (FCC) phase and it appeared as each cerium site is surrounding by eight oxygen sites and each oxygen sites has tetrahedron cerium sites in FCC arrangement [8].

Many literatures are available which reported the electrical, optical properties and structure of CeO<sub>2</sub> films using various deposition techniques such as reactive DC magnetron sputtering, electron beam evaporation, spray

pyrolysis, thermal evaporation, laser ablation deposition and pulsed- laser deposition [9,10]. Among the different methods, spray pyrolysis was mainly used because of low cost and its simplicity to produce large-area, well adherence films and easy doping with desirable composition [11,12].

Pure and doped CeO<sub>2</sub> thin film is suitable for various applications in optoelectronic devices which is attributed to the transparent oxide film, having absorption in the visible and near-IR region. CeO<sub>2</sub> films are widely used in the semiconductor, electrochromic device, gas sensor, counter electrodes, magnetic materials and solid oxide fuel cells (SOFC) [13-14]. It has many other potential applications as photocatalysis materials and in gas sensors for high oxygen storage capacity. Because of release oxygen easily and its ability to absorb, the CeO<sub>2</sub> thin films used as solid oxide fuel cells. Besides, at a lower temperature, it has higher ionic conductivity [15-17].

This paper reports the preparation of CeO<sub>2</sub> thin films on glass substrates using SPT. The effect of molarity concentration on the structural, morphological and optical properties are investigated in detail.

## 2 Materials and Methods

The thin film of cerium oxide (CeO<sub>2</sub>) is prepared by SPT.

\*Corresponding author E-mail: [faten.kassid@sci.utq.edu.iq](mailto:faten.kassid@sci.utq.edu.iq)

Firstly, the hepta-hydrate cerium chloride ( $\text{CeCl}_3 \cdot 7\text{H}_2\text{O}$ ) aqueous solution is prepared with different molarity, from 0.01, 0.03, 0.05, 0.1 to 0.2 M, by dissolving it in double-distilled water. Before starting spraying the solution on the substrate, the substrate is cleaned properly and anneal at 373 K to remove water molecules. It consists of liquid precursor with atomization metal salts and nozzles for droplet transport on to a heated substrate. On the substrate surface, decomposition and solvent evaporation result in the formation of the thin film.

The preheated substrate is maintained at a temperature of 623 K. The compressed air is used as carrier gas for spraying. The distance between substrate and nozzle is about 30 cm. The  $\text{CeCl}_3 \cdot 7\text{H}_2\text{O}$  solution is sprayed at spray rates of 2ml/min on to the glass substrate. The SPT exhibits good adherence with the substrate surfaces for the  $\text{CeO}_2$  films.

"The structure of  $\text{CeO}_2$  films are examined with X-ray diffractometer (Bruker, Germany) using  $\text{CuK}\alpha$  radiation (40kV and 30mA). The surface morphology of  $\text{CeO}_2$  thin films is examined by scanning electron microscope (SEM, Hitachi Model, 700 AT)". The optical absorption and transmittance characteristics are determined with UV-Vis-IR spectrophotometer (V-1200, UV-1600PC) in the wavelength range of 300-900 nm.

### 3 Results and Discussion

#### 3.1. X-Ray Diffraction

Figure 1 shows the XRD patterns of  $\text{CeO}_2$  films with different molarity of solution prepared at 623 k deposited on the glass substrate. XRD patterns of  $\text{CeO}_2$  films exhibits single phase with a cubic fluorite structure. The pattern of  $\text{CeO}_2$  film agrees with the JCPDS data 34-0394. It is also clear from the XRD spectrum that the variation in the molarity of solution in the range of 0.01 to 0.05 M leads to the formation of well-crystallized  $\text{CeO}_2$  which is strongly oriented along the (111) plane [1,16]. The diffractions peaks of all samples located at 28.2, 32.6, 46.8, 55.6, 58.8, 68.2 and 76.4 can be indexed to the (111), (200), (220), (311), (222), (400) and (331) plans of a cubic fluorite structure, respectively as shown in Table 1

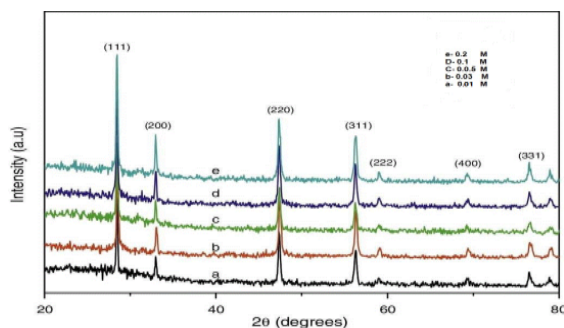


**Fig. 1.** XRD patterns of  $\text{CeO}_2$  films prepared with different molar concentration

**Table 1.** XRD analyses parameters for  $\text{CeO}_2$  film

| hkl planes        | 111  | 200  | 220  | 311  | 222  | 400  | 331  |
|-------------------|------|------|------|------|------|------|------|
| 2 $\theta$ (deg.) | 28.2 | 32.6 | 46.8 | 55.6 | 58.8 | 68.2 | 76.4 |

Scherer's formula used to calculate crystallite size from XRD data is given as,

$$D = \frac{K\lambda}{\beta \cos\theta} \dots \dots \dots (1) [18]$$

"where  $\lambda$  is the wavelength of the X-ray, D,  $\beta$  represent the crystallite size, and full-width half maximum of diffraction peak, respectively".

Some parameters like microstrain ( $\epsilon$ ), lattice constant and density of dislocation ( $\delta$ ) of the films are calculated with different molarity and are listed in Table 2. The following equations were used to calculate dislocation density ( $\delta$ ) and micro-strain ( $\epsilon$ ) respectively

The change in the molar concentration results in getting different size of  $\text{CeO}_2$  crystallites size. The size of all crystallites is in the nanometer range.

$$\delta = \frac{1}{D^2} \dots \dots \dots (2) \quad [18]$$

$$\epsilon = \frac{\beta \cos\theta}{4} \dots \dots \dots (3) \quad [18]$$

From Table 1, the dislocation density and lattice parameter is increased with a decreasing in the crystallite size. One of the general experimental facts is that the lattice parameters show expansion with reduction in particle size for nanoparticles of oxides while the nanoparticles of metal exhibit a lattice contraction. This lattice expansion with concentration variation is attributed to the strain of lattice, which is induced by the increase of  $\text{Ce}^{3+}$  ions because of the formation of oxygen vacancies [19].

**Table.2** Density of dislocation, micro-strain and lattice parameters of the thin films with different molar concentrations

| Mole concentration | Thickness | D nm | Dislocation density( $\times 10^{14}$ ) | Micro-strain ( $\times 10^{-4}$ ) | Lattice Constant ((Å)) |
|--------------------|-----------|------|---|-----------------------------------|------------------------|
| 0.01               | 83        | 108  | 0.71                                    | 0.056                             | 5.399                  |
| 0.03               | 103       | 98   | 0.85                                    | 0.37                              | 5.435                  |
| 0.05               | 132       | 71   | 1.56                                    | 0.81                              | 5.439                  |
| 0.1                | 178       | 89   | 1.43                                    | 0.053                             | 5.441                  |
| 0.2                | 201       | 92   | 0.84                                    | 0.048                             | 5.449                  |

### 3.2 Scanning Electron Macroscopy

Fig. 2 shows the SEM image of CeO<sub>2</sub> thin films at 623 K. It reveals that the film prepared with 0.01 and 0.03 M concentrations show spherical shaped particles with some voids. The film formed exhibits uniformity, smoothness, crack-free and high adhesion to the glass substrate. The smooth uniform surface of film depends on the molar concentration as the lower concentration produced rough surface up to 0.05 M and when the molarity is increased,

smoothness of thin-film increased and also some cracks have appeared on the surface. The formation of microcracks is observed in the 0.1 and 0.2 M concentration, which is primarily due to the thermal stress[20].

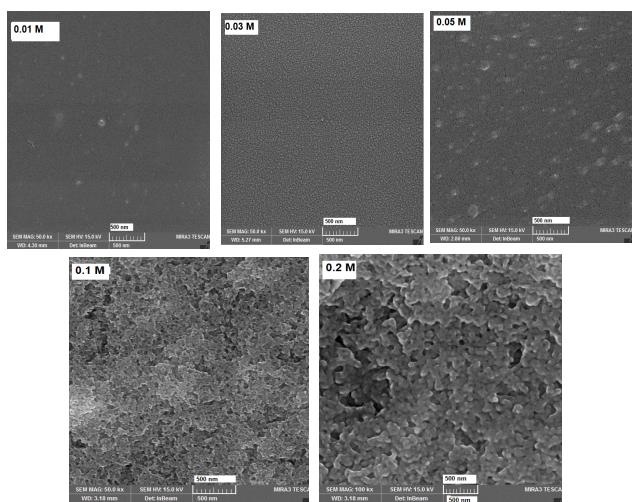


**Fig.2** SEM images for CeO<sub>2</sub> thin films with different molar concentration

### 3.3. Transmittance spectrum near infrared

Figure 3 shows transmittance spectra of CeO<sub>2</sub> films with thickness of 98, 110, 112, 114 and 120 nm, depending on the molarity of solution. The prepared films are mainly transparent in the visible which near infrared regions indicate that the films are uniform and have well adherence to the glass substrates. It is observed that the transmission decreases with increasing in molar concentration"[21].

The molarity effects on transmittance is reflected as, on increasing the molar concentration in turn reduces transmittance which is attributed due to the bonding between oxygen and cesium ion as covalent bonds [19]. Furthermore, the incident light transmittance is decreased at shorter wavelengths. So the outer orbits electrons were transferred to the higher energy levels to occupy vacant position of energy bands.

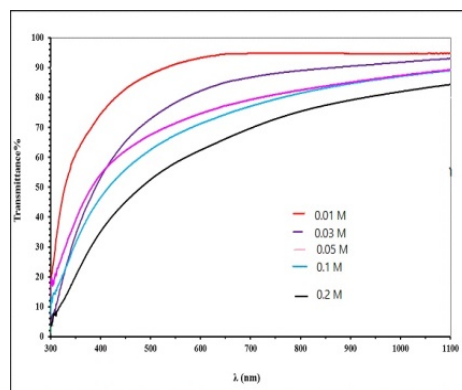


**Fig. 3** Transmittance spectrum of CeO<sub>2</sub> thin films with different concentration

### 3.4 absorption coefficient

The absorbance coefficient spectra of cerium oxide thin films prepared with various molarity are shown in figure 4. The spectra of absorption coefficient decreased with increasing wavelength and it exhibits high absorption coefficient value in UV region and constant in the visible region and near infrared regions. When the molar concentration increased, the absorbance spectra increasing up to 0.1 M, and then decreases because of the increase in pore size [21].

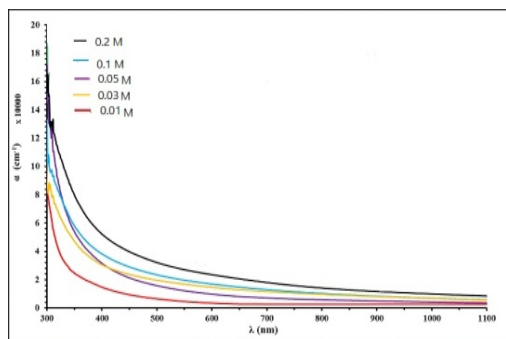


**Fig. 4** Absorption coefficient  $\alpha$  of  $\text{CeO}_2$  thin film with different molar concentration

### 3.5. Extinction Coefficient

The extinction coefficient ( $k$ ) of the  $\text{CeO}_2$  films is calculated using the relation  $k = \alpha\lambda/4\pi$  where  $\lambda$  is the wavelength and  $\alpha$  is the absorption coefficient. The results are shown in figure 5. The observed value of  $k$  is high for the wavelength range from 325 nm to 400 nm and is low in the higher range of wavelength from 450 nm to 1100 nm

The refractive index of the films with 0.01 M to 0.2 M found to be 1.193, 1.23, 1.29, 1.42 and 1.56, respectively. It is found that refractive index of the films decreases with an increase in the wavelength. The increase in refractive index for 0.05 M films suggests that the films are more absorbing than other mole concentration of the films. It may be attributed to the smaller crystal size at 0.05 M, which allows for closer packing, which is in good agreement with SEM observations [22].

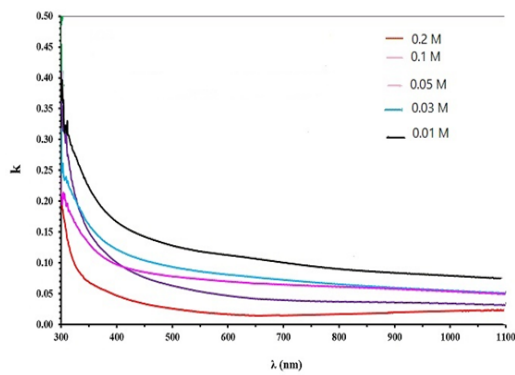


**Fig. 5** Extinction coefficient vs wavelength for  $\text{CeO}_2$  thin films with different concentration

### 3.6. Optical Energy Gap

The incident photon energy ( $h\nu$ ) depicted with  $(\alpha h\nu)^2$  as shows in Figure 6. It is observed that the optical energy gap decreased with the increase of crystallite size (98-120 nm) due to the size effect, the concentration of  $\text{Ce}^{3+}$  ions and oxygen vacancies [18].

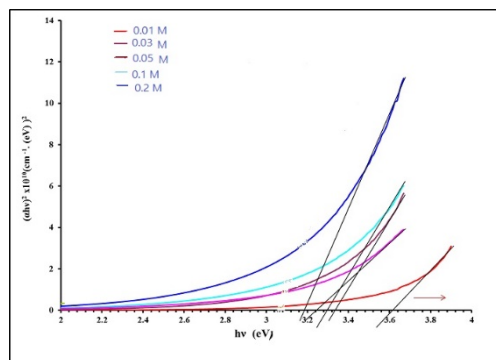


**Fig. 6** Variation in  $(\alpha h\nu)^2$  vs  $h\nu$  for  $\text{CeO}_2$  with different molar concentration

## 4 Conclusion

The  $\text{CeO}_2$  films were deposited on glass substrates with various molar concentration 0.01-0.2 M. The films deposited by spray pyrolysis technique is done by  $\text{CeCl}_3 \cdot 7\text{H}_2\text{O}$  as precursor. The XRD studies revealed the formation of polycrystalline ceria of cubic fluorite structure with the crystallite orientation preferred along (111) plane direction. The morphological analysis revealed that the particles are distributed uniformly on the surface and are confirmed through SEM. The UV-Visible spectra reveal that the films are transparent (70%) in the visible region and the bandgap is found to be in the range of 3.4 eV to 3.65 eV. Due to its nano-crystalline nature, the deposited  $\text{CeO}_2$  thin films can be used for various applications.

## References

- [1] R. Murugan, G. Vijayaprashath, P. Sakthivel, DAE solid state physics symposium, AIP Conf. Proc. 173, 080029-1-080029-3, (2016).
- [2] G. Balakrishnan, Arun Kumar Panda, C. M. Raghavan, Akash Singh, M. N. Prabhakar, E. Mohandas, P. Kuppasami, Jung Il Song, Journal of Materials Science: Materials in Electronics, **30**, 17, pp.16548–16553, 2019.
- [3] Hamed A. Gatea “The role of substrate temperature on the performance of humidity sensor manufactured from cerium oxide thin films” Journal of Materials Science: Materials in Electronics 31 (24), 22119-

- 22130.
- [4] K. Maniammal, Navas I, R. Vinod Kumar, IRJER, **4(9)**, (2017), [www.irjet.net](http://www.irjet.net)
- [5] ChetouiAbdelmounaim, Zouaoui Amara, AyatMaha , Materials Science in Semiconductor Processing , **43**:241-221, (2016).
- [6] ChunyanLv, Chen Zhu, Canxing Wang, Yahan Gao, Applied physics Letters, **106**:141102, (2015).
- [7] Zuwei Zhang, Chenguo Hu, YanfengXiong, Rusen Yang, Nanotechnology, **18**:465504, (2007).
- [8] CH.S.S. Pavan Kumar, R. Pandeewari, B.G. Jeyaprakash Journal of Alloys and Compounds,602,pp. 180-186,( 2014).
- [9] Hamed A. Gatea ,Iqbal S. Naji, Ameer F. Abulameer “Humidity Sensing Properties of Ferroelectric Compound Ba<sub>0.7</sub>Sr<sub>0.3</sub>TiO<sub>3</sub> Thin Films Grown by Pulsed Laser Deposition” International Journal of Thin Films Science and Technology,Vol. 9, No. 2, 143-150 (2020).
- [10] Y. J. Acosta-Silva, M. Toledano-Ayala, G. Torres-Delgado, I. Torres-Pacheco, A. Méndez-López, Hindawi Journal of Nanomaterials” **2019**, Article ID 5413134,8pages,(2019).
- [11] Preetam Singh, K. M. K. Srivatsa , Sourav Das, Advance Materials letters, **6(5)**:371-376, (2015).
- [12] Hamed A. Gatea “Synthesis and characterization of BaSrTiO<sub>3</sub> perovskite thin films prepared by sol gel technique” International Journal of Thin Film Science and Technology,10, 2, 5,2021.
- [13] Hamed A. Gatea “Effect of Substrate-induced Strains on Ferroelectric and Dielectric Properties of Lead Zirconate Titanate Films Prepared by the Sol-gel Technique” Nanoscience & Nanotechnology-Asia, Vol. 11. No.3, pp 322-329,2021.
- [14] K KBabitha, A Sreedevi, K P Priyanka , BobbySabu, Indian journal of Pure & Applied physics, **53**,596-603, (2015).
- [15] Chunjie Wang, Int. J. Appl. Ceram. Technol, **12**,S1:E142-E148, (2015).
- [16] R Pandeewari , B G Jeyaprakash, Bull. Mater. Sci., **37(6)**, 1293-1299,(2014)
- [17] Sher Bahadar Khan, M. Faisal, Mohammed M. Rahman, KalsoomAktar, Int. J. Electrochem. Sci. ,**8**, ,7284-7297,(2013).
- [18] Hamed A Gatea, Rajaa K Mohammad, Sarah M Khali, “Impact of Annealing Temperature on Optical Properties of CeO<sub>2</sub> Thin Films Deposition by Spin Coating Technique” 2022 International Congress on Human-Computer Interaction, Optimization and Robotic Applications (HORA), IEEE,1-3, 2022.
- [19] R. Suresh, V. Ponnuswamy, R. Mariappan Applied surface science, **273**, pp. 457-464,(2013)
- [20] Reza Zamiri, Hossein Abbastabar, Ajay Kaushal, AzmiZakaria, Pols ONE journal, **10(4)**,(2014).
- [21] Hamed A. Gatea, “Effect of High Temperature on Thermal Analysis, Structure and Morphology of CeO<sub>2</sub> Nanoparticles Prepared by Hydrothermal Method” International Journal of Thin Films Science and Technology,11,2 ,201, 2022.
- [22] Ka Wang Yongqin Chang Liang Lv Yi Long,applied surface science,**15**, (2015).